Simulating sea ice in the Arctic Ocean and Eastern Siberian Sea

Ayumi Fujisaki Manome[1] and Jia Wang[2]
University of Michigan[1],
NOAA Great Lakes Environmental Research Laboratory[2]
4840 S. State Rd, Ann Arbor, MI 48108 USA
ayumif@umich.edu, jia.wang@noaa.gov

This study conducts ice-ocean coupled simulations for the Arctic Ocean, with the nested region of the Eastern Siberian Sea with 4km horizontal resolution. The ocean model is based on the Princeton Ocean Model. The ice dynamic model is based on the elastic-viscous-plastic rheology and the ice thermodynamics is based on the one-dimensional 0-layer model. These models are fully parallelized using the Message-Passing Interface. Initial conditions for ocean and sea ice, as well as atmospheric forcing, are provided by NCEP Climate Forecast System Reanalysis. The simulation will ultimately incorporate data assimilation of hydrographic data from the Russian-American Long-term Census of the Arctic (RUSALCA) cruises. The study will present an initial hindcast simulation from 2000 to 2015 with basic model validation based on comparison with satellite observations.

1 Introduction

The extent of Arctic sea ice reached its all time low in September 2012, shattering all previous record lows since satellite record-keeping began 33 years ago (Serreze et al. 2007; Comiso et al. 2008; Stroeve et al. 2012) including the previous record low in September 2007. The Arctic sea ice extent was about 20% less in September 2012, when it was 3.41×10^6 km^2, compared to September 2007, when it was 4.3×10^6 km^2. If Arctic summer sea ice continues to decline at this rate, which is much faster than any climate models predict (Stroeve et al. 2012), but a conservative estimate based on recent empirical data, then the Arctic summer is expected to become ice free by ~ 2040. Should this occur, then society must be prepared to mitigate and adapt to the impacts caused by this unprecedented change in the Arctic environment.

For example, as a result of diminishing Arctic sea ice that reduces the meridional air temperature gradient and weakens the westerly jet stream (i.e., becomes more unstable with larger meanderings), cold winter and extreme winter weather events have become more frequent over the northern North Atlantic and Eurasia (Francis and Vavrus 2012; Wu et al. 2013), which further strengthens the declining trend of winter surface air temperature (SAT) over Eurasia (Honda et al. 2009). The cause of this accelerated decline of summer sea ice was thought to be 1) the combined effects of Arctic Oscillation (AO)-induced and greenhouse gas-induced thermal warming (Wang and Ikeda 2000; Rigor et al. 2002), 2) the cumulative effects of ice/ocean albedo positive feedback, 3) the increase of Arctic clouds and water vapor (Ikeda et al. 2003; Stroeve et al. 2012), and 4) the anomalously increasing meridional wind forcing associated with the Dipole Anomaly (DA) pattern (Wang et al. 2009; Ogi and Wallace 2012; Overland et al. 2012).

Since 1995, the decline in summer Arctic sea ice has accelerated, without any obvious increasing trends in either cyclone activity (Serreze et al. 2007) or total net solar radiation. At the same time, while there is some evidence suggesting a weak link between the AO and rapid sea ice retreat during recent years, the AO index has been highly variable, shifting among positive, neutral, and mostly negative states (Wang et al. 2009).

Although accelerated sea ice melting has been attributed to Arctic temperature amplification associated with the positive ice-ocean albedo and ice-cloud feedback processes (Ikeda et al. 2003), this is clearly not the whole story behind the rapid sea ice decline. Wang et al. (2009) invoked the DA to explain the complete series of intermittent ice minima observed in 1995, 1999, 2002, 2005, 2007, and 2008. Clearly, an improved quantitative understanding is needed to explain the recently observed, unprecedented loss of sea ice (Stroeve et al. 2012).

In this study, we configure an ice-ocean coupled model to the entire Arctic Ocean to investigate the mechanisms of why and how summer sea ice melts at the fastest rate in the Pacific Arctic (hot spot). Our further target is to assimilate existing and on-going hydrographic data and moorings over the nested region of the East Siberian Sea (ESS) and Chukchi Sea. Here we present our initial results of pan-Arctic simulations results.

2 Model

The ice-ocean coupled model developed in this study is based on a three-dimensional high-resolution regional model in the Arctic Ocean (De Silva et al. 2015), The ocean model is based

on the Princeton Ocean Model (POM; Mellor et al. 2002) with a generalized vertical coordinate system. The ice thermodynamics model is based on the zero-layer thermodynamic model (Semtner, 1976). The ice dynamic model is based on the elastic-viscous-plastic (EVP) rheology (Hunke and Dukowicz, 1997; Hunke, 2001) with the effect of ice floe collision (Sagawa and Yamaguchi, 2006; Sagawa, 2007). To avoid the numerical instability triggered by the sudden increment of ice strength at near 100% ice concentration, De Silva et al. (2015) modified the formulation of ice strength so that the regime of ice strength smoothly switches from the floe collision rheology to the traditional Hibler-type formulation at 90% ice concentration.

The horizontal advection in the ice model is based on a semi-Lagrangian method (Sagawa and Yamaguchi, 2006; Sagawa, 2007), where sub-grid location of a rectangular ice bunch is defined in a cell. This method has advantage in reducing numerical diffusion of ice mass in comparison with the Eulerian advection (Sagawa, 2007).

The model is forced by hourly atmospheric forcings; winds, air temperature, specific humidity, cloud cover, sea level air pressure, and precipitation. These forcings are provided from the NCEP Climate Forecast System Reanalysis (CFSR, Saha et al. 2010), except for precipitation that is from climatological data from the NCEP NCAR re-analysis. The initial conditions for oceanic temperature, salinity, current speeds are provided from CFSR. The lateral boundary conditions for temperature and salinity is specified from the Polar science center Hydrographic Climatology (PHC) version 3.0.
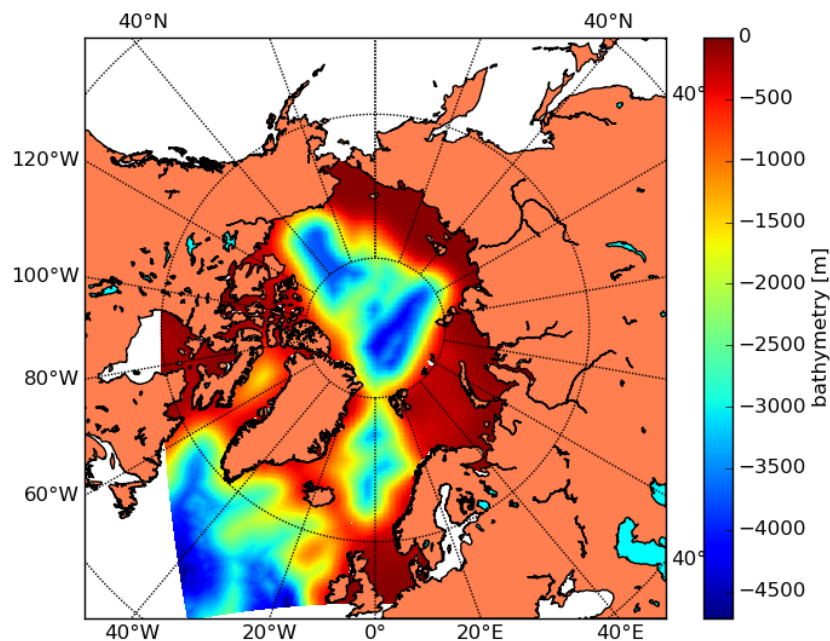

Figure 1. Model domain and bathymetry. The model boundaries coincide with the edges of topography contour

The model topography is shown in Figure 1 and is based on the Earth Topography 1 Arc-minute Gridded Elevation Dataset (ETOPO1). The model includes the freshwater inputs from 13 major rivers, whose discharge data is listed at the website of the Arctic Ocean Model Intercomparison Project (AOMIP) and is from Prange (2002). The initial test simulation period is from September 1999 to August 2000, while the planned simulation period is up to 2015 or present. For model validation, we use the time series of ice area from NASA's Arctic/Antarctic Sea Ice Time Series and monthly ice concentration maps from the National Snow & Ice Data Center, both of which are derived from satellite passive-microwave sensors, specifically Special Sensor Microwave Imagers (SSMIs) for the period of our simulation.

3   Results

The model was run for several years with the same annual cycle of atmospheric forcing from September 1999 to August 2000. After five years, we observe that the three-dimensional current, water temperature, salinity, and ice volume achieved near-equilibrium. This relatively fast time to reach an equilibrium state is likely due to the fact that the model is initiated from the snapshot of three-dimensional current (u and v), temperature (T), and salinity (S) from CFSR.

Figure 2 shows the time series of ice area after a 5-year spin-up both from the simulation results and the observation with SSMIs. The annual cycle is captured while the simulation result has some overshooting after March and the observed minimum of ice area in September is somehow overestimated. This overshooting was also observed in the application of ICEPOM to the Laurentian Great Lakes (Manome and Wang, in preparation) and was improved by using a multi-category ice thickness distribution model with ridge parameterization that was implemented in a Los Alamos Sea Ice Model (CICE)-based ice model. This is likely because the single category ice thickness model in ICEPOM tends to produce thinner ice than the CICE-based ice model does.

Figure 3 shows the annual mean ice motion and ice thickness. The signal of the Beaufort Gyre and the Transport Drift Stream can be observed although the Transpolar Drift Stream crossing near the north pole seems somewhat weak compared with the schematic currents suggested in the Arctic Monitoring and Assessment Programme (AMAP, 1998). Figure 4 shows the monthly mean ice motion and ice concentration in September 1999 and March 2000. Both the simulation results and the satellite-based observation with SSMIs are shown. Seasonal variation is reasonably reproduced. On the other hand, the simulated ice cover is excessive in the East Siberian Sea in summer (September) and in the northeast of Iceland in winter (March). The discrepancy between the simulated and observed ice cover in the Eastern Siberian Sea is problematic as, ultimately, this our area of interest for the future nested simulation. This error is likely related to the weak Transpolar Drift Stream, which should carry the ice in the Eastern Siberian Sea out. If this is the case, one possible way to avoid this error is to conduct the nested simulation with the lateral boundary conditions directly from CFSR, not from our ICEPOM outputs.

4   Summary

This paper presented the initial results of our ice-ocean coupled simulations for the Arctic Ocean using ICEPOM. While the overall seasonal variation of ice condition is reproduced reasonably in comparison with the satellite-based observations, there are some local discrepancies with the observations. In our initial plan, the next step will be a continuous run in the subsequent years up to 2015, as well as to conduct nested simulations for the Eastern Siberian Sea with spatial resolution of 1-3 km. However, another option could be to go directly to the nested region that covers the Eastern Siberian Sea, which is our ultimate interest. This way we can start from a downscaled snapshot and lateral boundary conditions from CFSR. Assuming CFSR provides near-true conditions of ice and ocean, this reduces uncertainties in the larger domain around the nested region as it can be fixed to the CFSR solution and we can only focus on small-scale processes of $\sim 10^{0}$ km in the nested region.

References

AMAP, 1998. AMAP Assessment Report: Arctic Pollution Issues. Arctic Monitoring and Assessment Programme (AMAP), Oslo, Norway. xii+859 pp.

Comiso, J.C., Parkinson, C.L., Gersten, R., and Stock, L., 2008. Accelerated decline in the Arctic sea ice cover, Geophys. Res. Lett., 35, L01703, doi:10.1029/2007GL031972.

De Silva, L.W.A, Yamaguchi, H., and Ono, J., 2015. Ice-ocean coupled computations for sea-ice prediction to support ice navigation in Arctic sea routes, Polar Research 2015, 34, 25008, http://dx.doi.org/10.3402/polar.v34.25008.

Francis, J.A., and Vavrus, S.J., 2012. Evidence linking Arctic amplification to extreme weather in mid-latitudes. Geophys. Res. Lett., 39, L06801, doi:10.1029/2012GL051000.

Honda, M., Inoue, J., and Yamane, S., 2009. Influence of low Arctic sea-ice minima on anomalously cold Eurasian winters. Geophys. Res. Lett., 36, L08707, doi:10.1029/2008GL037079.

Hunke, E.C., 2001. Viscous_plastic sea ice dynamics with the EVP model: linearization issues. Journal of Computational Physics 170, pp. 18-38.

Hunke, E.C., and Dukowicz J.K., 1997. An elastic_viscous_plastic model for sea ice dynamics. Journal of Physical Oceanography, 27, pp. 1849-1867.

Ikeda, M., Wang, J., and Makshtas, A., 2003. Importance of clouds to the decaying trend in the Arctic ice cover. J. Meteorol. Soc. Japan, 81, 179-189.

Manome, A., and Wang, J., Simulating hydrodynamics and ice cover in Lake Erie using an unstructured grid model, in preparation.

Ogi, M., and Wallace, J. M., 2012. The role of summer surface wind anomalies in the summer Arctic sea ice extent 2010 and 2011. Geophys. Res. Lett., 39, L09704, doi:10.1029/2012GL051330.

Overland, J.E., Francis, J.A., Hanna, E., and Wang, M., 2012. The recent shift in early summer Arctic atmospheric circulation, Geophys. Res. Lett., 39, DOI: 10.1029/2012GL053268

Prange, M., 2002. Einfluss arktischer S"u"swasserquellen auf die Zirkulation im Nordmeer und im Nordatlantik in einem prognostischen Ozean-Meereis-Modell. Ph.D. thesis, University of Bremen, Bremen, Germany.

Rigor, I.G., Wallace, J.M., and Colony, R.L., 2002. Response of Sea Ice to the Arctic Oscillation. J. Climate, 15, 2648–2663. doi: http://dx.doi.org/10.1175/

Sagawa, G., 2007. Development of ice dynamic model that takes account of floe collision and its validation in numerical sea ice forecast in the Sea of Okhotsk. (In Japanese.) PhD thesis, University of Tokyo.

Sagawa, G., and Yamaguchi H., 2006. A semi-Lagrangian sea ice model for high resolution simulation. In J.S. Chung (ed.): Proceedings of the Sixteenth International Offshore and Polar Engineering Conference. pp. 584_590. Cupertino, CA: International Society of Offshore and Polar Engineers.

Saha, S., Moorthi, S., Pan, H.L., Wu, X., Wang, J., Nadiga, S., et al. 2010. The NCEP climate forecast system reanalysis. Bulletin of the American Meteorological Society, 91, pp. 1015-1057.

Semtner A.J., 1976. A model for the thermodynamic growth of sea ice in numerical investigations of climate. Journal of Physical Oceanography 6, pp. 379-389.

Serreze, M.C., Holland, M.M., and Stroeve, J., 2007. Perspectives on the Arctic's shrinking sea ice cover. Science, 315, 1533, doi:10.1126/science.1139426.

Stroeve, J.C., Serreze, M.C., Holland, M.M., Kay, J.E., Maslanik, J., and Barrett, A.P., 2012. The Arctic's rapidly shrinking sea ice cover: A research synthesis, Climatic Change, 110:1005–1027, DOI 10.1007/s10584-011-0101-1.

Wang, J. and Ikeda, M., 2000. Arctic Oscillation and Arctic Sea-Ice Oscillation. Geophys. Res. Lett., 27(9) 1287-1290.

Wang, J., Zhang, J., Watanabe, E., Mizobata, K., Ikeda, M., Walsh, J.E., Bai, X., and Wu, B., 2009. Is the Dipole Anomaly a major driver to record lows in the Arctic sea ice extent? Geophys Res. Lett, 36, L05706, doi:10.1029/2008GL036706.

Wu, B., Handorf, D., Dethloff, K., Rinke, A., and Hu, A., 2013. Winter Weather Patterns over Northern Eurasia and Arctic Sea Ice Loss, Mon. Wea. Rev. (in press).
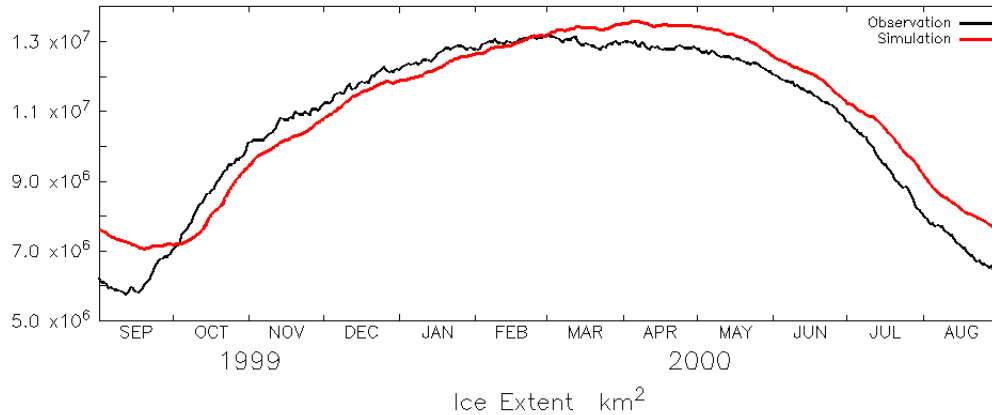
Figure 2. Time series of ice extent from September 1999 to August 2000. Black line is of the satellite-observed ice extent from NASA's Arctic/Antarctic Sea Ice Time Series (http://neptune.gsfc.nasa.gov/csb/index.php?section=59). Red line is from the simulation results.
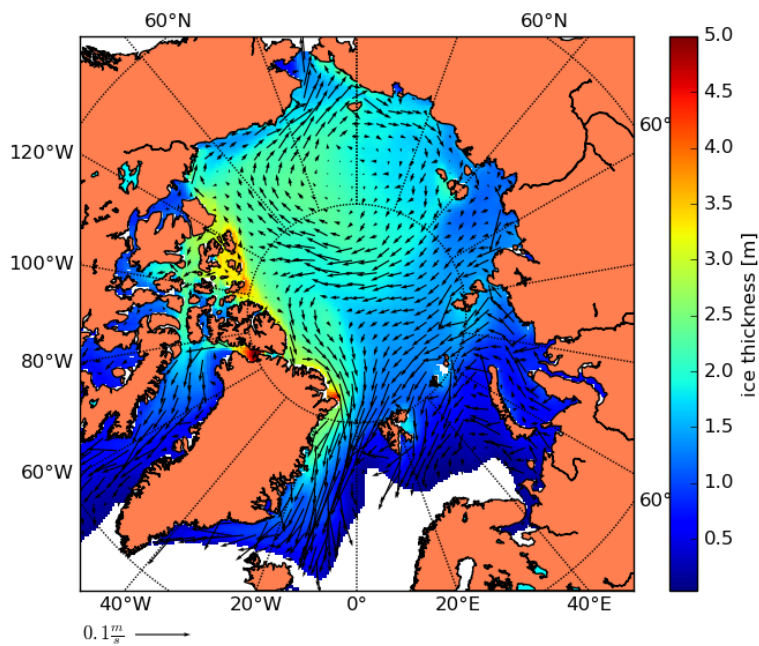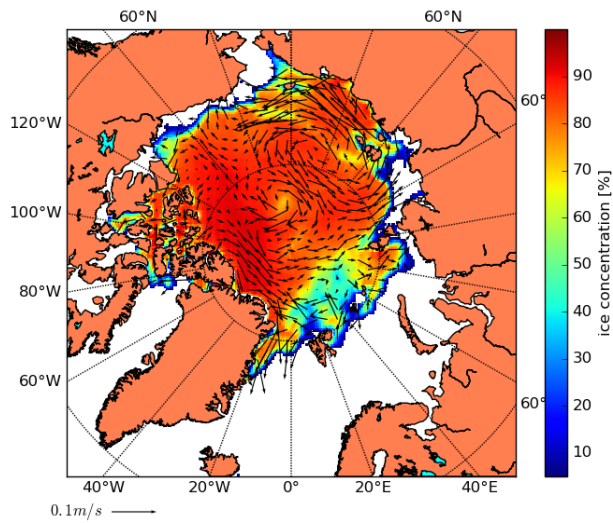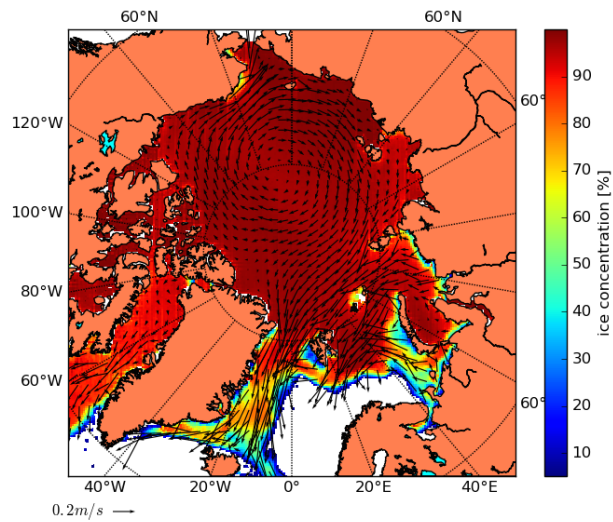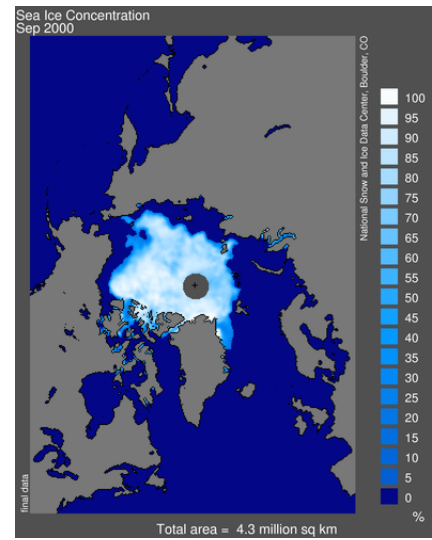

Figure 3. Annual mean ice motion (vector) and ice thickness (shading) from September 1999 to August 2000. From the ICEPOM simulation results.
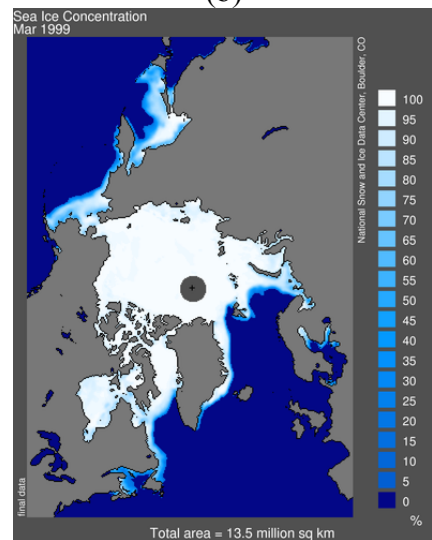
(a) September, 1999

(b)

(c) March, 2000

(d)

Figure 4. Monthly mean ice motion (vector) and ice concentration (shading) in September 1999 and March 2000. (a) and (c): The ICEPOM simulation results. (b) and (d): The observation.